Vol. 30, No. 7 Journal of Semiconductors July 2009

Characterization of GaN grown on 4H-SiC and sapphire by Raman spectroscopy and high resolution XRD*

Duan Huantao(段焕涛)†, Gu Wenping(谷文萍), Zhang Jincheng(张进成), Hao Yue(郝跃), Chen Chi(陈炽), Ni Jinyu(倪金玉), and Xu Shengrui(许昇瑞)

(Key Laboratory of Fundamental Science for National Defense on Wide Band-Gap Semiconductor Technology, School of Microelectronics, Xidian University, Xi'an 710071, China)

Abstract: The crystal quality, stress and strain of GaN grown on 4H-SiC and sapphire are characterized by high resolution X-ray diffraction (HRXRD) and Raman spectroscopy. The large stress in GaN leads to the generation of a large number of dislocations. The Raman stress is determined by the results of HRXRD. The position and line shape of the A_1 longitudinal optical (LO) phonon mode is used to determine the free carrier concentration and electron mobility in GaN. The differences between free carrier concentration and electron mobility in GaN grown on sapphire and 4H-SiC are analyzed.

Key words: metalorganic vapor phase epitaxy; GaN; Raman; XRD

DOI: 10.1088/1674-4926/30/7/073001 **PACC:** 6588; 7280E

1. Introduction

GaN has attracted considerable research interest in recent years because of its use in a wide range of applications, including blue/ultra-violet light emitting devices, ultra-violet detectors[1, 2], as well as electronic devices, such as field-effect transistors (FETs) and bipolar transistors[3–5]. Up to now, the GaN material has often been epitaxially grown on foreign substrates, such as sapphire, SiC, and Si, because of the lack of a large native substrate. The lattice constant mismatch of GaN with sapphire and SiC is –13% and +4%, respectively[6]. This mismatch leads to impractically small critical layer thickness values and ideal heteroepitaxy has not been observed. Layers grown on these substrates are dense with threading and edge dislocations. On the other hand, the thermal expansion coefficient in the basal plane of GaN differs significantly from those of SiC and sapphire[7, 8]. Consequently, the high-temperature deposition process used in all epitaxial growth of GaN results in thermal stress upon cooling to room temperature, providing the material does not relax by cracking or on account of a very high dislocation density. The biaxial stress observed in epitaxial GaN is a consequence of the lattice constant and the thermal mismatch strain[9, 10]. Also, it is well known that GaN exhibits high unintentional n-type doping levels due to residual oxygen donors introduced during the heteroepitaxy[11, 12]. This effect is particularly evident in GaN-on-sapphire epitaxy, where oxygen can be incorporated directly from the substrate. This high level of background n-doping is detrimental to both the electronic device properties and the effective doping control in an optical device.

Stress can modulate the band-gap of GaN films[13, 14], and consequently, the optical properties. Extremely large values of stress can produce cracks in these films. Therefore, the ability to examine stress in epilayers is essential to the film growth and the device fabrication. The most direct approach for the analysis of strain in epitaxial GaN is through a high resolution X-ray diffraction (XRD) measurement. The (0002) diffraction peak is used to determine the *c*-axis lattice constant. Another accepted approach for obtaining the biaxial stress in epilayers is by using Raman spectroscopy[15]. In GaN, the shift in the E_2 (high) symmetry phonon energy, from the value exhibited by unstressed material, is proportional to the stress. Raman spectroscopy also can be employed for the determination of the free-carrier concentration in GaN. In polar semiconductors, longitudinal optical (LO) phonon modes couple strongly with plasmons through the macroscopic electric field. LO phonon plasmon (LPP) coupled modes have been observed in doped GaN materials and the LPP frequencies are very sensitive to and can be used as a probe of the free-carrier concentration[16]. With this principle, Ponce *et al.* demonstrated how Raman spectroscopy can be used to probe the carrier concentration[17]. The free-carrier concentration determined by Raman scatting from an analysis of the LPP coupled mode in GaN has also been reported by Kozawa *et al.*[18].

In this study, epilayers grown on both sapphire and 4H-SiC substrates are examined and their biaxial compressive and tensile stress states are studied by using Raman spectroscopy. Plasmon-phonon coupling is exploited to estimate the carrier concentration of GaN grown on sapphire and 4H-SiC.

---

* Project supported by the Key Program of National Natural Science Foundation of China (No. 60736033), the National Key S & T Special Project (No. 2008ZX0101002-003), the National Defense Scientific and Technical Pre-Research Program of China (Nos. 51311050112, 51308030102, 51308040301).

† Corresponding author. Email: htduan@163.com

Received 30 December 2008, revised manuscript received 24 February 2009

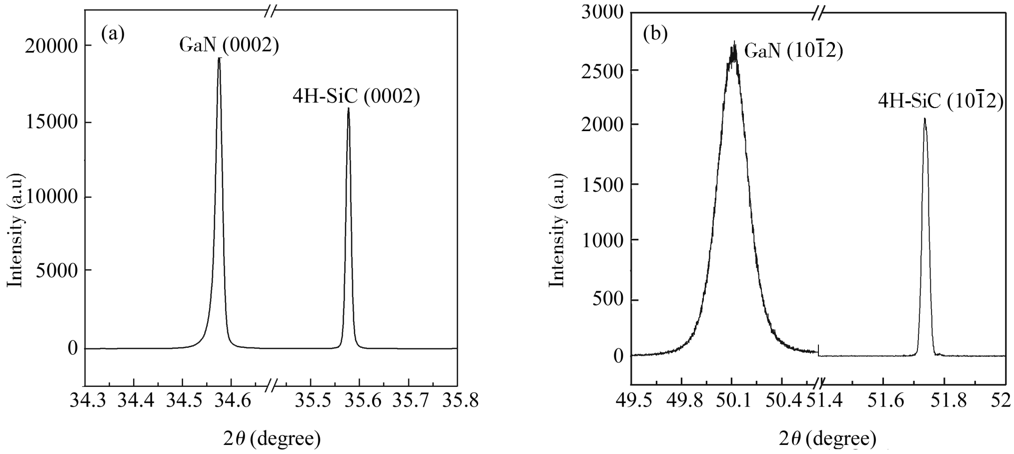

Fig. 1. (a) XRD patterns of GaN-(0002) grown on 4H-SiC; (b) XRD patterns of GaN-(10$\bar{1}$2) grown on 4H-SiC.

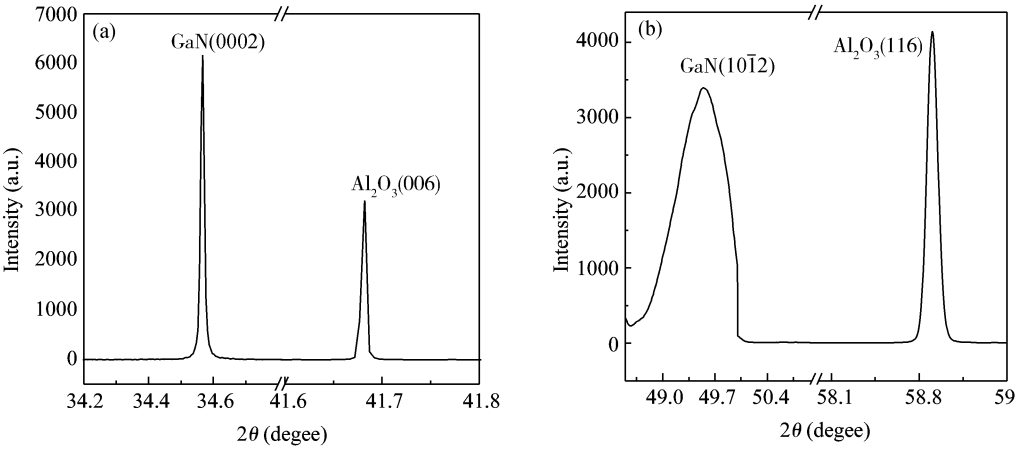

Fig. 2. (a) XRD patterns of GaN-(0002) grown on Al_2O_3; (b) XRD patterns of GaN-(10$\bar{1}$2) grown on Al_2O_3.

2. Experiment

Two sets of GaN epilayers grown by a low-pressure MOCVD system were studied. In the first set of GaN grown on (001) sapphire, an epilayer was initiated by a thin (20 nm) AlN buffer layer grown on the substrate at a low temperature (620 °C). The substrate temperature was then elevated to 1000 °C to grow the subsequent GaN epilayers. The second set of samples was grown on 4H-SiC substrates at a temperature of 1000 °C. High temperature (HT) AlN of 30 nm was used as a buffer layer. Hydrogen was used as the carrier gas. Triethylgallium (TEGa), trimethylaluminum (TMAl), and ammonia (NH_3) were used as precursors.

Micro-Raman spectroscopic measurements were carried out at room temperature using a 514 nm line of Ar^+ laser as the excitation source. The resolution was 1 cm^{-1}. The Raman measurements were performed in back-scattering Z(X,-)Z geometry, in which the E_2 (high) and A_1(LO) mode are Raman active.

In the XRD measurements, a commercial system with a Ge(220), four-fold, bartel-type monochromator and a Ge(220) three-fold analyzer was used to make 2theta–omega scans and omega rocking curves. To measure the lattice constants of GaN, reflections of the Cu$K\alpha_1$ line from (0002) in the symmetrical mode and (10$\bar{1}$2) planes in the asymmetrical mode were measured. The strain components along the *c* axis (ε_{zz}) and along the $a = b$ axis (ε_{xx}) were calculated.

3. Results and discussion

3.1. XRD

The *c*-axis and *a*-axis lattice constants of GaN grown on 4H-SiC were 0.51907 and 0.31886 nm, respectively, calculated from the results, as shown in Fig. 1. Obtained from Fig. 2, the lattice constants of GaN grown on sapphire were c = 0.51850 nm and a = 0.31901 nm.

The strain components ε_{zz} and ε_{xx} are calculated. The Poisson ratio was obtained from

$$\varepsilon_{zz}/\varepsilon_{xx} = -2\nu/(1-\nu), \tag{1}$$

and the biaxial stress σ was obtained from

$$\varepsilon_{xx} = \frac{1-\nu}{E}\sigma_{xx}, \tag{2}$$

$$\varepsilon_{zz} = \frac{1-\nu}{E}\sigma_{zz}, \tag{3}$$

where E is Young's modulus. The Poisson ratio gave excellent consistency with the average value of $\nu = 0.26$. This agrees well with published values of the Poisson ratio[19, 20]. The values of the stress of GaN grown on SiC and sapphire calculated using our Poisson ratio and Young's modulus of E = 290 GPa

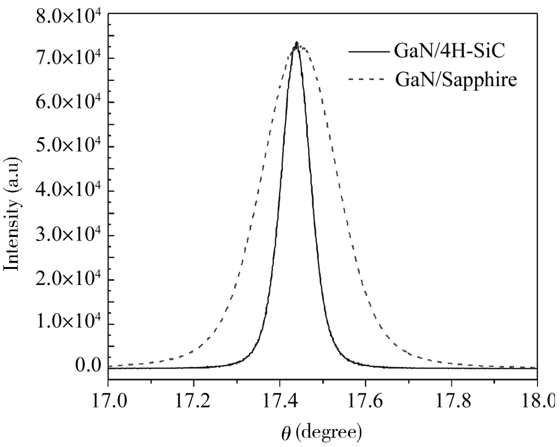

Fig. 3. GaN-(0002) rocking curve of XRD patterns for GaN grown on 4H-SiC and sapphire.

from Refs. [9, 19] were 0.15 GPa and 0.39 GPa, respectively.

The crystal quality was characterized by the full-width at half maximum (FWHM) of X-ray rocking curves (XRC). It has been demonstrated that the XRC for the symmetric (0002)-reflecting plane is related to screw and mixed dislocations, whereas the XRC for asymmetric $(10\bar{1}2)$-reflecting plane is directly influenced by all threading dislocations, including edge dislocations[21]. As shown in Fig. 3, the crystal quality of GaN grown on 4H-SiC was obviously better than that grown on sapphire. This refers only to the preferred lattice constant match between GaN and 4H-SiC.

3.2. Raman scattering

GaN has a hexagonal structure belonging to the C_{6v} symmetry group and, thus, from theory, two A_1, two E_1, two E_2 and two B_1 phonon modes are predicted. The zone-center phonon frequencies of hexagonal GaN calculated by Karch *et al.* are: E_2 (low) 143 cm^{-1}, B_1 (low) 337 cm^{-1}, A_1 transverse optical (TO) 541 cm^{-1}, E_1 (TO) 568 cm^{-1}, E_2 (high) 579 cm^{-1}, B_1 (high) 720 cm^{-1}, A_1 (LO) 748 cm^{-1}, E_1 (LO) 757 cm^{-1}. Among these phonon modes, one A_1, one E_1 and two E_2 modes are Raman active. According to the Raman selection rule and for the Z(X,-)Z configuration used in this study, the A_1 (LO), E_2 (high) and E_2 (low) modes had been expected to be observed in the Raman spectra. However, the E_2 (low) mode is not within the covered spectral range of the present observation mode.

Stress in epitaxial GaN (0001) is biaxial. The GaN E_2 (high) value of 567.2 cm^{-1}[22] was used as the stress-free reference, and the Raman shift $\Delta\omega$ from the phonon energy of the unstressed material was related to the biaxial stress. Figure 4 shows the red and blue shift of E_2 (high) phonons due to compressive stress (GaN grown on sapphire) and tensile stress (GaN grown on 4H-SiC), respectively. The relationship between the strain and the Raman shift can be written as $\sigma = \Delta\omega / k_R$, where k_R is the Raman stress factor. Using $E = 290$ GPa and $v = 0.26$ obtained by XRD results, our value of the GaN Raman stress factor was –4.4 cm^{-1}/GPa. This value is in the range of published values of –2.7[23], –4.1[24], –6.2[25], and –7.7 cm^{-1}/GPa[26]. A relationship between the Raman shift and the stress from XRD measurements is established. It is known that the incorporation of impurities and point defects significantly reduces the phonon lifetime, thus broadening the Raman line-width. The FWHM of E_2 (high) Raman modes of GaN grown on sapphire and 4H-SiC are 4.5 cm^{-1} and 3 cm^{-1} respectively, indicating that a larger number of defects and impurities had been incorporated into the GaN grown on sapphire. The results of the Raman measurement agreed well with those of XRD, as shown in Fig. 4. This also indicates that Raman spectroscopy is a valuable tool in the characterization of epilayer crystalline quality.

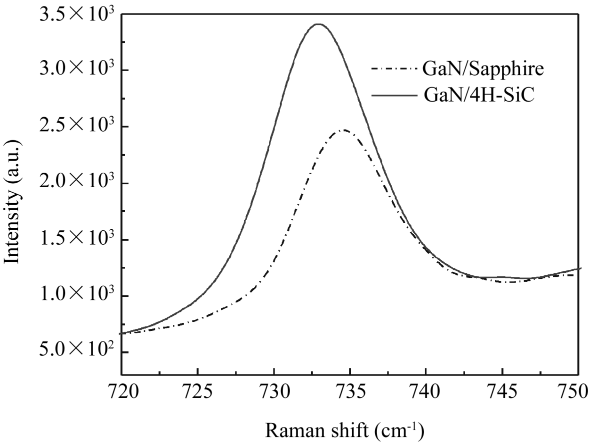

Fig. 4. Raman spectra of the A1 (LO) phonon mode of GaN grown on 4H-SiC and sapphire.

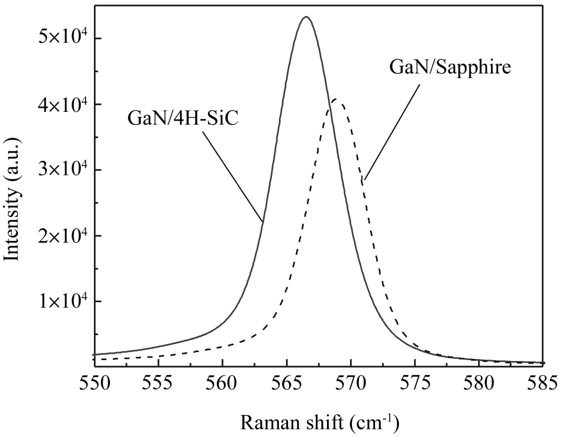

Fig. 5. Raman spectra of the E_2(high) phonon mode of GaN. Blue shift results from compressive stress (GaN/sapphire) and red shift is from tensile stress (GaN/4H-SiC).

The Raman E_2 (high) mode in GaN is not directly affected by the free-carrier concentration. As shown in Fig. 4, the A_1 (LO) phonon mode of GaN grown on 4H-SiC had a blue shift of 3 cm^{-1} when compared with that of GaN grown on sapphire, as shown in Fig. 5. It is known that the high-frequency branch of the LPP coupled mode shifts slightly to the high frequency side, with accompanying peak shape broadening. It also should be noted that a biaxial compress stress of 1 GPa could shift the A_1 (LO) peak towards a higher wave number by 0.8 cm^{-1}[27]. Note that this is a factor of 5 less than the shift of the E_2 (high) mode for the same biaxial stress. The peak shift of the A_1 (LO) mode by stress was negligible based on the results obtained by XRD. Therefore, the carrier density can be evaluated by a line-shape fitting analysis based on a semi-classical model, which involves consideration of the deformation potential and the electro-optical mechanisms. The line shape of the LO phonon is given by Refs. [28–30]

$$I(\omega) = SA(\omega)\mathrm{Im}\left[\frac{-1}{\varepsilon(\omega)}\right], \tag{4}$$

where S is a proportionality factor,

$$A(\omega) = 1 + 2C\omega_{\mathrm{T}}^2 \frac{\omega_{\mathrm{P}}^2\gamma(\omega_T^2 - \omega^2) - \omega^2\mathit{\Gamma}(\omega^2 + \gamma^2)}{\Delta} + \frac{C^2\omega^4}{\Delta}\frac{\omega_{\mathrm{P}}^2\gamma(\omega L^2 - \omega_{\mathrm{T}}^2) + \mathit{\Gamma}(\omega_{\mathrm{P}}^2 - 2\omega^2) + \omega^2\mathit{\Gamma}(\omega^2 + \gamma^2)}{\omega_{\mathrm{L}}^2 - \omega_{\mathrm{T}}^2}, \tag{5}$$

and Δ is given by

$$\Delta = \omega_{\mathrm{P}}^2\gamma[(\omega_{\mathrm{T}}^2 - \omega^2)^2 + (\omega\mathit{\Gamma})^2] + \omega^2\mathit{\Gamma}(\omega_{\mathrm{L}}^2 - \omega_{\mathrm{T}}^2)(\omega^2 + \gamma^2), \tag{6}$$

where C is the Faust-Henry coefficient, ω_{P} is the plasma frequency , and ω_{T} and ω_{L} are the TO and LO phonon frequencies. $\mathit{\Gamma}$ and γ are the phonon and plasmon damping constants, respectively. The Faust-Henry coefficient can be deduced from the ratio of the intensity of the LO and TO phonon peaks in undoped GaN using the following equation:

$$\frac{I_{\mathrm{L}}}{I_{\mathrm{T}}} = \left(\frac{\omega_0 + \omega_{\mathrm{L}}}{\omega_0 + \omega_{\mathrm{T}}}\right)^4 \frac{\omega_{\mathrm{T}}}{\omega_{\mathrm{L}}}\left(1 + \frac{\omega_{\mathrm{T}}^2 - \omega_{\mathrm{L}}^2}{C\omega_{\mathrm{T}}^2}\right), \tag{7}$$

where ω_0 is the frequency of the laser.

$$\varepsilon(\omega) = \varepsilon_\infty\left(1 + \frac{\omega_{\mathrm{L}}^2 - \omega_{\mathrm{T}}^2}{\omega_{\mathrm{T}}^2 - \omega^2 - i\omega\Gamma} - \frac{\omega_{\mathrm{P}}^2}{\omega^2 - i\omega\gamma}\right). \tag{8}$$

The A_1(LO) coupled modes of GaN epitaxy were fitted according to Eqs. (1)–(5), with ω_{T}, ω_{L}, and C being fixed at literature values of $\omega_{\mathrm{T}} = 533$ cm^{-1}, $\omega_{\mathrm{L}} = 735$ cm^{-1}, and $C = 0.48$[31]. For the case of GaN, values of $\varepsilon_\infty = 5.35$ and $m^* = 0.2m_0$ were adopted[32]. $\mathit{\Gamma}$, γ, and ω_{P} were treated as the fitting parameters. The free carrier concentration n can be calculated using

$$\omega_{\mathrm{p}} = \left(\frac{4\pi ne^2}{\varepsilon_\infty m^*}\right)^{1/2}, \tag{9}$$

where n is the free carrier concentration and m^* is the effective mass of the carriers. The mobility of the free carriers can be obtained by

$$\gamma = \frac{e}{m^*\mu}. \tag{10}$$

The plasma frequencies for the GaN grown on 4H-SiC and sapphire were 40 cm^{-1} and 115 cm^{-1}, and the carrier concentration of GaN grown on 4H-SiC and sapphire were found to be 1.91×10^{16} cm^{-3} and 1.57×10^{17}cm^{-3}, respectively. The results indicated that the free carrier concentration in GaN grown on sapphire was higher than that on 4H-SiC. The origin of the residual donors in GaN grown on sapphire is presumably oxygen impurities diffused from the substrate[33, 34]. The plasma damping constant was obtained from line shape analysis. The electron mobilities in GaN grown on 4H-SiC and sapphire calculated using Eq. (7) were 130 cm^{-2}/(V·s) and 73 cm^{-2}/(V·s), respectively. The electron mobility in GaN grown on 4H-SiC was found to be higher than that on sapphire, which was manifested as a larger plasmon damping in GaN grown on sapphire. As shown in Fig. 3, the dislocation density in GaN grown on 4H-SiC is lower than that in GaN grown on sapphire. It is believed that the observed difference in plasmon damping is a result of the difference in the dislocation density.

4. Summary

We correlated independent measurements of strain and stress on GaN grown on 4H-SiC and sapphire. The lattice constants of GaN along the *a*-axis and the *c*-axis were obtained by HRXRD. The strain along the *a*-axis and the *c*-axis was also calculated by using published lattice constants for unstrained GaN. We obtained the GaN Poisson ratio $v = 0.26$ using these strain values. The values of stress of GaN grown on SiC and sapphire calculated using our Poisson ratio and Young' modulus of $E = 290$ GPa were 0.15 GPa and 0.39 GPa, respectively. This refers only to the preferred lattice constant match between GaN and 4H-SiC. The results obtained by HRXRD also agreed well with those obtained by Raman spectroscopy. The crystal quality of GaN was characterized by Raman spectroscopy and HRXRD; these results obtained by these two different methods also agreed well with each other. That demonstrates that Raman spectroscopy is a valuable tool in the characterization of epilayer crystalline quality and residual strain. A Raman stress factor of –4.4 cm^{-1}·GPa^{-1} was deduced by XRD measurements. Consequently, the values of stress in GaN can be obtained expediently and quickly by Raman spectroscopy in the future. Moreover, the free carrier concentrations and electron mobilities were deduced from an analysis of the longitudinal optical phonon-plasmon coupled mode. The carrier concentrations of GaN grown on 4H-SiC and sapphire were found to be 1.91×10^{16} cm^{-3} and 1.57×10^{17} cm^{-3}, respectively. We can see that the important origin for unintentional n-type doping of GaN grown on sapphire is the diffusion of O atoms from the sapphire. The differences between the electron mobilities in GaN grown on 4H-SiC and sapphire are also analyzed. All in all, as a new characterization method, Raman spectroscopy is a valuable tool in the quick and expedient characterization of the epilayer crystalline quality, the residual strain, and the electrical characteristics.

References

[1] Bhapkar U V, Shur M S. Monte Carlo calculation of velocity-field characteristics of wurtzite GaN. J Appl Phys, 1997, 82:

1649

[2] Zhen X Q, Kun X Q, Kuwano S, et al. Growth mode and surface reconstruction of GaN (001) thin films on 6H-SiC. Chin Phys B, 2001, 10:157

[3] McCarthy L S, Kozodoy P, Rodwell M J W, et al. AlGaN/GaN heterojunction bipolar transistor. IEEE Electron Device Lett, 1999, 35: 277

[4] Chumbes E M, Smart J A, Prunty T, et al. Microwave performance of AlGaN/GaN metal insulator semiconductor field effect transistors on sapphire substrates. IEEE Trans Electron Devices, 2001, 48: 416

[5] Khan M A, Shur M, Kuznia J N, et al. Temperature activated conductance in GaN/AlGaN heterostructure field effect transistors operating at temperatures up to 300 °C. Appl Phys Lett, 1995, 66: 1083

[6] Ponce F A, Bour D P, Gotz W, et al. Homoepitaxy of GaN on polished bulk single crystals by metalorganic chemical vapor deposition. Appl Phys Lett, 1996, 68: 917

[7] Kirchner V, Heinke H, Hommel D, et al. Thermal expansion of bulk and homoepitaxial GaN. Appl Phys Lett, 1997, 77: 1434

[8] Numerical data and functional relationships in science and technology, new series Group 3, Vol. 17, Part a. New York: Springer, 1982

[9] Oh E, Lee S K, Park S S, et al. Optical properties of GaN grown by hydride vapor-phase epitaxy. Appl Phys Lett, 2001, 78: 273

[10] Neugebaur J, van de Walle C G. Atomic geometry and electronic structure of native defects in GaN. Phys Rev B, 1994, 50: 8067

[11] Wetzel C, Suski T, Ager J W, et al. Pressure induced deep gap state of oxygen in GaN. Phys Rev Lett, 1997, 78: 3923

[12] Look D C, Molnar R J. Degenerate layer at GaN/sapphire interface: influence on Hall-effect measurements. Appl Phys Lett, 1997, 70: 3377

[13] Gil B. Gallium nitride II, Vol 57. Pankove J T, Moustakas T D, ed. Academic Boston, 1997

[14] Rieger W, Metzger T, Angerer H, et al. Influence of substrate-induced biaxial compressive stress on the optical properties of thin GaN films. Appl Phys Lett, 1996, 68: 970

[15] Liu R, Cave N. SiGeC alloys and their applications. Pantelides S, Zollner S, ed. New York: Gordon and Breach, 2002

[16] Perlin P, Camassel J, Knap W, et al. Investigation of longitudinal-optical phonon-plasmon coupled modes in highly conducting bulk GaN. Appl Phys Lett, 1995, 67: 2524

[17] Ponce F A, Steeds J W, Dyer C D, et al. Direct imaging of impurity-induced Raman scattering in GaN. Appl Phys Lett, 1996, 69: 2650

[18] Kozawa T, Kachi T, Kano H, et al. Raman scattering from LO phonon-plasmon coupled modes in gallium nitride. J Appl Phys, 1994, 75: 1098

[19] Polian A, Grimsditch M, Grzegory I. Elastic constants of gallium nitride. J Appl Phys, 1996, 79: 3343

[20] Wachman J B Jr, Tefft W E, Lam D E Jr, et al. Elastic constants of synthetic single-crystal corundum at room temperature. J Res Natl Bur Stand, 1960, 64A: 213

[21] Heying B, Wu X H, Keller S, et al. Role of threading dislocation structure on the X-ray diffraction peak widths in epitaxial GaN films. Appl Phys Lett, 1996, 68: 643

[22] Nootz G, Schulte A, Chernyak L, et al. Correlations between spatially resolved Raman shifts and dislocation density in GaN films. Appl Phys Lett, 2002, 80: 1355

[23] Davydov V Y, Averkiev N S, Goncharuk I N, et al. Raman and photoluminescence studies of biaxial strain in GaN epitaxial layers grown on 6H-SiC. J Appl Phys, 1997, 82: 5097

[24] Kisielowski C, Kruger J, Ruvimov S, et al. Strain-related phenomena in GaN thin films. Phys Rev B, 1996, 54: 17745

[25] Kozawa T, Kachi T, Kano H, et al. Raman scattering from LO phonon-plasmon coupled modes in gallium nitride. J Appl Phys, 1994, 75: 1098

[26] Lee I, Choi I, Lee C, et al. Stress relaxation in Si-doped GaN studied by Raman spectroscopy. J Appl Phys, 1998, 83: 5787

[27] Demangeot F, Frandon J, Renucci M A, et al. Raman determination of the phonon deformation potentials in α-GaN. Solid State Commun, 1996, 100: 207

[28] Klein M V, Ganguly B N, Colwell P J. Theoretical and experimental study of Raman scattering from coupled LO-phonon-plasmon modes in silicon carbide. Phys Rev B, 1972, 6: 2308

[29] Irmer G, Toporov V V, Bairamov B H, et al. Determination of the charge carrier concentration and mobility in n-gap by Raman spectroscopy. Phys Status Solidi B, 1983, 119: 595

[30] Hon D T, Faust W L. Dielectric parameterization of Raman lineshapes for GaP with a plasma of charge carriers. Appl Phys, 1973, 1: 241

[31] Barker A S Jr, Ilegems M. Infrared lattice vibrations and free-electron dispersion in GaN. Phys Rev B, 1973, 7: 743

[32] Faust W L, Henry C H. Mixing of visible and near-resonance infrared light in GaP. Phys Rev Lett, 1996, 17: 1265

[33] Wetzel C, Suski T, Ager J W, et al. Pressure induced deep gap state of oxygen in GaN. Phys Rev Lett, 1997, 78: 3923

[34] Look D C, Molnar R J. Degenerate layer at GaN/sapphire interface: influence on Hall-effect measurements. Appl Phys Lett, 1997, 70: 3377